A Truncated Model for
Finite Amplitude Baroclinic Waves in a Channel

Zhiming Kuang

1 Introduction

To date, studies of finite amplitude baroclinic waves have been mostly numerical. The numerical models, ranging from general circulation models (GCMs) to two-layer quasi-geostrophic (QG) models have been able to simulate certain observed features of the mid-latitude synoptic system quite well. For instance, the asymmetric life cycle of global normal modes observed by Randel and Stanford [1] has been well simulated by Simmons and Hoskins [2] with a primitive equation model and by Feldstein and Held [3] with a 2-layer QG model. Coherent wave packets that are observed in both the Northern Hemisphere (NH) and the Southern Hemisphere (SH) have also been simulated in a hierarchy of models [4, 5]. Analytical theories of finite amplitude baroclinic waves, on the other hand, have not been developed except for those under weakly nonlinear conditions. The requirement of small super-criticality severely limits the application of such a theory on the real atmosphere, which clearly exhibits finite super-criticality.

This work attempts to construct a truncated 2-layer QG model that is capable of capturing the essential features of finite amplitude baroclinic waves. The existence of such a model is suggested by the remarkably simple meridional structures of the nonlinear baroclinic waves as simulated by untruncated 2-layer QG models [5]. Successful truncation may provide insight into the underlying processes, and might lead a step towards an analytical theory for the finite amplitude barolinic waves.

2 Model

The 2-layer QG equations on a β-plane may be written as follows:

$$\frac{\partial q_1}{\partial t} + J(\psi_1, q_1) = r \left(\frac{\psi_1 - \psi_2}{2} - \tau_e \right) - \nu \nabla^6 \psi_1 \tag{1}$$

$$\frac{\partial q_2}{\partial t} + J(\psi_2, q_2) = -r \left(\frac{\psi_1 - \psi_2}{2} - \tau_e \right) - \kappa_M \nabla^2 \psi_2 - \nu \nabla^6 \psi_2 \tag{2}$$

where

$$q_j = \beta y + \nabla^2 \psi_j + (-1)^j \left(\frac{\psi_1 - \psi_2}{2} \right), \; j = 1, 2 \tag{3}$$

Here, j = 1 and 2 refer to the upper and lower layers. κ_M is the Ekman friction, r is the relaxation rate towards the equilibrium state τ_e, ν is the numerical diffusion that parameterizes cascade to unresolved scales. The equations have been nondimensionalized. The radius of deformation λ is chosen as the horizontal length scale, where

$$\lambda^2 = g(\rho_2 - \rho_1)H/(2\rho_2 f_0^2) \tag{4}$$

and H is the depth of either layer. Time is scaled by λ/U_0, where U_0 is the horizontal velocity scale. For more detailed discussion about this model, the reader is referred to Lee and Held (1993) [5].

I choose the boundary conditions that correspond to a channel with rigid walls [6]:

$$\frac{\partial \psi_j}{\partial x} = 0 \ \& \ \overline{\frac{\partial \psi_j}{\partial y}} = 0 \quad y = 0, L_y \tag{5}$$

x is the direction along the channel (zonal, longitude) and y is the direction across the channel (meridional, latitude). This choice is supported by the fact that wave packets are more coherent when the storm track is more meridionally confined. The general solution that satisfies the boundary conditions can be written as follows:

$$\psi_j(x, y, t) = \quad \sum_{m=1}^{\infty} A'_{j,m}(x, t) \sin \frac{my}{N} \quad + \sum_{n=1}^{\infty} C_{j,n}(t) \cos \frac{ny}{N}$$

$$+ \sum_{m=1}^{\infty} \overline{A_{j,m}}(t)(\sin \frac{my}{N} - \frac{my}{N} \quad + [(m \bmod 2) - 1]\frac{m}{N}\frac{y^2}{N\pi}) \tag{6}$$

where $A'_{j,m}(x, t) = A_{j,m}(x, t) - \overline{A_{j,m}}$. The overbar denotes the average over x. I have chosen L_y to be $N\pi\lambda$.

3 "Rules" for Truncation

To construct a truncated model, one needs to first select a desirable subset of base functions, then express the unknowns in terms of these base functions and substitute them into the equations. One then projects the equations onto the selected base functions to obtain a new set of equations to solve for the coefficients of the base functions.

To be "desirable", first of all, the truncation needs to be simple, as the whole goal of truncation is simplification, or to capture essential features of the system with less degrees of freedom. It is also desirable for the truncated models to retain the conservation laws of, for example, energy, potential enstrophy, and momentum. Even though they are not required, as the truncated models are, by nature, approximations, conservation laws, if retained, prove to be very useful for model validation and facilitate the discussion of, for instance, the energy conversion.

It can be shown that if energy and potential enstrophy, or in general, any quadratic quantities, are conserved for a base function set, they are also conserved by a subset that consists of orthogonal base functions. One complete set of base functions, suggested by the general solution (6), includes:

$$()' \sin \frac{my}{N}, \ m = 1, \infty \tag{7}$$

$$\overline{()}(\sin\frac{my}{N} - \frac{my}{N} + [(m \bmod 2) - 1]\frac{m}{N}\frac{y^2}{N\pi}), \ m = 1, \infty \tag{8}$$

$$\overline{()}\cos\frac{ny}{N}, \ n = 1, \infty \tag{9}$$

Modes in set 7 may be called eddy base functions and have zero x averages. Set 8 and 9 consists of base functions that represent the zonal mean components. As $\int_0^{N\pi}\sin\frac{my}{N}\sin\frac{ly}{N}dy = 0$, when $m \neq l$, and $\int ()'\overline{()}dx = 0$ by definition, every base function in (7) is orthogonal to all the other base functions, including those in (8) and (9). Base functions in (9) are orthogonal to other base functions within set 9 yet not orthogonal to base functions in set 8. Base functions in set (8) are not orthogonal to each other. Therefore, any combination of set 7 base functions together with any combination of set 9 base functions or one set 8 base function would be an orthogonal set. Here, I choose set 9 to represent the zonal mean components as it appears to be simpler than set 8.

When there is no friction, the untruncated model should conserve total momentum

$$\frac{d}{dt}\int_0^{N\pi}\frac{\partial\overline{\psi_M}}{\partial y}dy = 0 \tag{10}$$

where subscript M denotes the barotropic component. Adding equation (1) and equation (2) gives

$$\frac{\partial q_M}{\partial t} + J(\psi_M, q_M) + J(\psi_T, q_T) = 0 \tag{11}$$

Subscript T denotes the baroclinic component. It is clear that changes in the zonal mean barotropic components can only come from wave-wave interactions represented by the Jacobian of eddies. Since the eddies have base functions of the form $()'\sin\frac{my}{N}$, if the indexes (m's) of any pairs of eddy base functions are separated by odd numbers and set 9 is selected as the base functions for the zonal components, it can be shown that the Jacobians in Eq. 11 do not affect the channel integrated barotropic zonal velocity, i.e. they conserve the total momentum (Appendix). The same is not true when set 8 is used or when the indexes of the eddy base functions are separated by even numbers. It directly follows that the selected eddy base function set should have no more than 2 base functions, for with more than 2 base functions, there must be at least one pair whose indexes are separated by an even number.

4 Truncation I

Following the "rules" described in the previous section,

$$\left\{ ()'\sin\frac{y}{N}, ()'\sin\frac{2y}{N}, \overline{()}\cos\frac{y}{N}, \overline{()}\cos\frac{2y}{N} \right\}, \tag{12}$$

appears to be an appropriate set. The unknown variables are then expressed in terms of these base functions.

$$\psi_j(x, y, t) = A'_{j,1}(x, t)\sin\frac{y}{N} + A'_{j,2}(x, t)\sin\frac{2y}{N} + \overline{C_{j,1}}(t)\cos\frac{y}{N} + \overline{C_{j,2}}(t)\cos\frac{2y}{N}$$
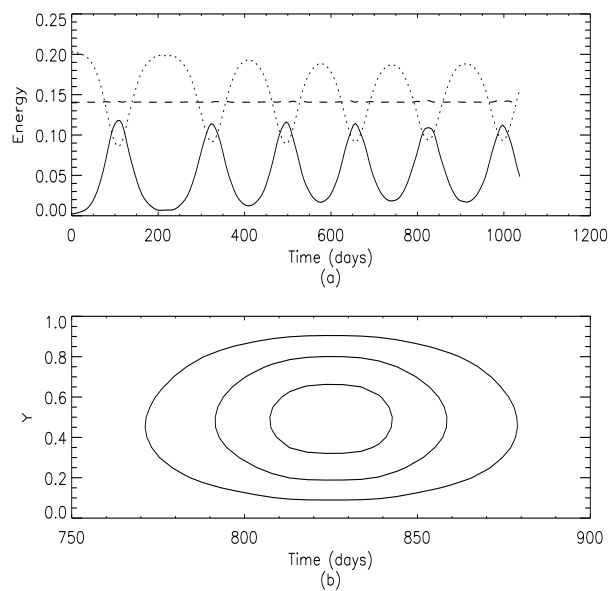
Figure 1: Time evolution of a normal mode with a weakly supercritical background zonal flow. (a) shows the total wave energy (solid), the baroclinic mean flow energy (dotted) and the barotropic mean flow energy (dashed). The absolute values of baroclinic mean flow energy have been shifted in the plot. (b) shows the latitude-time contour of zonally averaged upper layer wave streamfunction squared (i.e. variance) over one lifecycle of the normal mode. The unit in the y direction is $2\pi\lambda$.

The prime over $A_{j,i}$s and the overbar over $C_{j,i}$s remind us that A represents deviations from the zonal average and C represents the zonal means (i=1,2). By Equation 3, q_j, excluding the βy term, can be expressed in terms of the following components:

$$()' \sin \frac{y}{N} : \quad \frac{\partial^2 A'_{j,1}}{\partial x^2} - \frac{A'_{j,1}}{N^2} + (-1)^j \frac{A'_{1,1} - A'_{2,1}}{2}$$

$$()' \sin \frac{2y}{N} : \quad \frac{\partial^2 A'_{j,2}}{\partial x^2} - \frac{4A'_{j,2}}{N^2} + (-1)^j \frac{A'_{1,2} - A'_{2,2}}{2}$$

$$\overline{()} \cos \frac{y}{N} : \quad -\frac{\overline{C_{j,1}}}{N^2} + (-1)^j \frac{\overline{C_{1,1}} - \overline{C_{2,1}}}{2}$$

$$\overline{()} \cos \frac{2y}{N} : \quad -\frac{4\overline{C_{j,2}}}{N^2} + (-1)^j \frac{\overline{C_{1,2}} - \overline{C_{2,2}}}{2}$$

After substituting ψ_j and q_j into equations 1 and 2, I project the equations onto the selected base functions. Take $\overline{()} \cos \frac{y}{N}$ as an example, the projection is done by first multiplying the equations by $\overline{()} \cos \frac{y}{N}$, and then integrating over y and averaging over x. Doing the projection for each base function and for both layers gives us 8 predictive equations for the 8 unknowns (the $A_{j,i}$s and $C_{j,i}$s). I then solve the new equations numerically using the spectral method. The nonlinear Jacobian terms are computed using the spectral transform method. As the spatial dimension of the problem is reduced from 2 to 1 (there is no y dependence in the equations now), the implementation is greatly simplified. I implement the model in a way that the selected base function set needs not to be the one specified in (12), but can be any combination of set 7 and set 9 base functions.

I will first study the nonlinear initial value problem for this truncated model, and then study the forced and dissipated system. The channel width is set to be 2π in this study.

4.1 Normal mode study

Without forcing and dissipation, I initialize the system with a zonal mean profile that is supercritical and perturb it with a $()' \sin \frac{y}{N}$ zonal wave disturbance that is close to the most unstable mode. The super-criticality and the most unstable mode are obtained from a linear stability analysis that I did for zonal wave disturbances with y dependence of the form $\sin \frac{my}{N}$ and zonal background flows of the form $\cos \frac{ny}{N}$ (both in terms of stream-function).

Normal mode evolution with a weakly supercritical zonal flow has been studied using the weakly nonlinear theory. Figure 1 shows the time evolution of a normal mode with a weakly supercritical background zonal flow calculated from the truncated model. The stream-function of the background flow takes the form of $\overline{()} \cos \frac{y}{N}$. As described by the weakly nonlinear theory and simulated by untruncated 2 layer QG models, there is little change in the barotropic zonal flow energy. The eddies grow baroclinically and also decay baroclinically, exhibiting a symmetric life cycle in terms of wave streamfunction squared.

In the real atmosphere, however, normal modes are observed to have asymmetric life cycles. This is not explained by the weakly nonlinear theory. For eddies to decay barotropically, some of the eddy energy has to be converted into barotropic mean flow energy through irreversible mixing processes like wave breaking. Figure 2 shows the time evolution of a normal mode in the untruncated model when the super-criticality is raised. Greater changes in
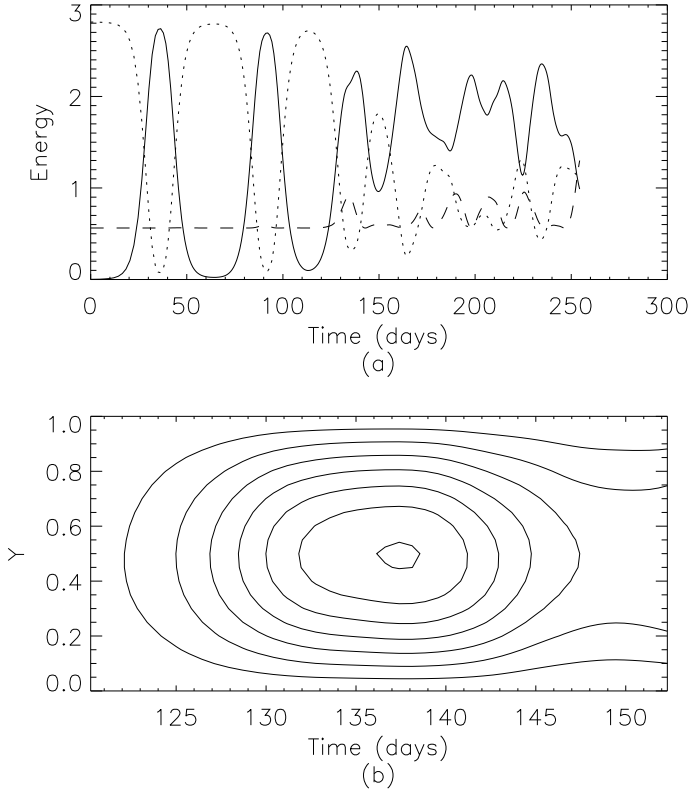
Figure 2: The same as Figure 1, except for the large super-criticality case.

the barotropic mean flow energy is observed. The life cycle becomes asymmetric as seen in the latitude-time contour of the zonal variance of the upper layer streamfunction. Changes in the barotropic mean flow energy are quite small however. So is the asymmetry of the life cycle. This should be expected since the truncated model has very limited degrees of freedom in the y direction, which limits its ability of mimicking fine scale processes like wave breaking. The model's ability of fully simulating the asymmetry in the eddy life cycles may be further limited by the $\cos \frac{y}{N}$ shape zonal mean stream-function that I have chosen. The resulted $\sin \frac{y}{N}$ shape zonal winds have rather weak meridional wind shear, which is thought to be critical for the barotropic decay of waves.

4.2   Forced and dissipated systems

I now examine the statistically steady state behaviors of finite amplitude wave when forcing and dissipation are present. The system is initialized with small noise like perturbations, with a Ekman friction κ_M of 0.05 and a relaxation time of 50 model days (i.e. r=0.02), and is relaxed towards the equilibrium profile τ_e. The relative magnitude of κ_M r, τ_e affects the shear strength of the statistically steady state. Here, I use the equilibrium profile τ_e, which takes the form of $\cos \frac{y}{N}$, as a parameter to change the super-criticality of the statistically steady state.

101
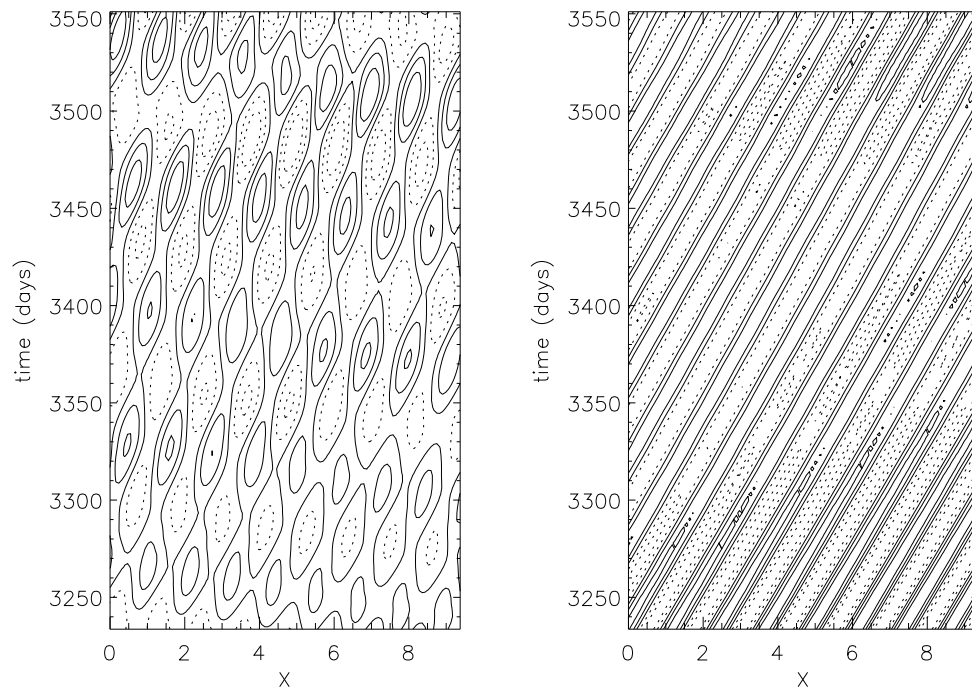
Figure 3: The longitude-time contour plots for the $\sin \frac{y}{N}$ (left) and $\sin \frac{2y}{N}$ (right) modes of the upper layer stream-function for the weak super-criticality case. The unit of x (longitude) is $2\pi\lambda$. Negative contours are dotted.
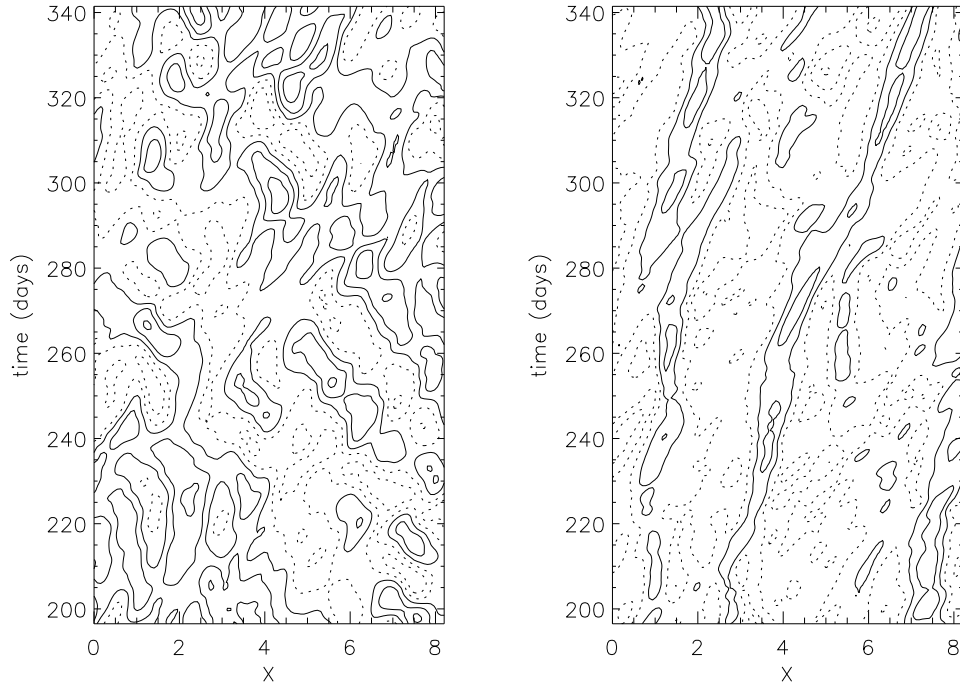
Figure 4: The same as figure 3, except for the strong super-criticality case.

The results from the truncated model are remarkably similar to those from an untruncated model study by Esler [7]. In Esler's study, the meridional structure is fully resolved by a 100 grid point finite differencing. An Empirical Orthogonal Function (EOF) analysis was then applied on the results to identify the dominant modes. Esler identified the first two modes as the antisymmetric mode and the symmetric mode, which have almost identical structures as the $\sin \frac{y}{N}$ and $\sin \frac{2y}{N}$ modes used in this study. This result is not totally expected since although the $\sin \frac{y}{N}$ and $\sin \frac{2y}{N}$ modes have the largest linear growth rates, whether they should still dominate when nonlinear effects become important is not totally clear. In figures 3 and 4, I present the longitude-time contour plots of the upper layer streamfunction for the cases of weak super-criticality (linear growth rate is about 0.02/day) and strong super-criticality (linear growth rate is about 0.17/day) respectively. For the weak super-criticality case, the wave train is modulated and the peaks appear to move at the same velocity as the phase speed. For the strong super-criticality case, the waves undergo quite chaotic evolution. Figure 3 may be compared to Esler's figure 15, and figure 4 may be compared to his figure 18. The remarkable similarity between the truncated model results and the untruncated model results strongly implies that the system has very low degrees of freedom in the meridional direction.

The model may be further reduced. Without the zonal mean component $\cos \frac{y}{N}$, one obtains results similar to those shown in figure 3 and 4 exceptthat the asymmetry of the eddy life cycles would not be simulated. Although not shown here, the potential vorticity (PV) fields in the upper and lower layers also resemble the results from Esler's study (his figure

19) and show the expected behaviors. The PV field in the lower layer is homogenized and the PV gradient in the upper layer is strengthened with some indication of wave breaking.

5 Other Truncations and Discussion

Esler's model [7] does not show coherent wave packets. However, wave packets were found over a broad parameter regime by Lee and Held in their 2-layer QG model [5]. The two differences between their model and Esler's model are: (1) Lee and Held used a wider channel (21λ) than Esler did ($2\pi\lambda$); (2) Lee and Held used a Gaussian zonal wind shear while Esler used a uniform zonal wind shear. These two differences appear to be crucial for wave packet formation.

It turns out that the wave packets are readily formed if wave-wave interaction only affects the mean flow and does not change the eddies. This is sometimes called the quasi-linear or wave-mean flow interaction model [3]. The simplest example of such a system has the following base function set:

$$\left\{ ()' \sin \frac{y}{N}, \overline{()} \cos \frac{y}{N} \right\}, \tag{13}$$

One can also choose, for example,

$$\left\{ ()' \sin \frac{y}{N}, ()' \sin \frac{2y}{N}, \overline{()} \cos \frac{y}{N} \right\}, \tag{14}$$

but ignore effects on the eddies by the wave-wave interaction, or choose, for example,

$$\left\{ ()' \sin \frac{3y}{N}, ()' \sin \frac{4y}{N}, \overline{()} \cos \frac{3y}{N} \right\}, \tag{15}$$

so that the wave-wave interactions do not project back onto the eddies themselves. Figure 5 shows the results for selection (13) as an example. The super-criticality here is much greater than that of the case in figure 4 (linear growth rate is about 1.9/day), yet wave packets are found and exhibit great coherence.

For the base function sets specified in (13), (14) and (15), the behavior of wave packets closely resembles that described in Lee and Held (1993) [5]. For example, the number of wave packets is found to increase with increasing super-criticality and increasing channel length. The power spectrum of the eddies is also found to be very simple, as found by Lee and Held for the wave packets (e.g. their figure 11) [5], while truncation (I) gives very noisy spectrum when the super-criticality is high.

In all the quasi-linear models, one eddy mode interacts with other eddy modes and with itself to affect the evolution of the mean flow (nonlinear). The evolution of the eddies, however, is determined by the wave-mean interaction and is not directly affected by the wave-wave interaction. In these cases, the evolution of an eddy mode is in a sense independent of the other modes (of course, eventually they are coupled through the mean flow). The role of this "independence" in wave packet formation is unclear. Furthermore, from a weakly nonlinear analysis [7] and from the difference between Esler's model and Lee and Held model, it appears that the eddies need to be confined away from the walls for wave packets to form. Further understanding of these two points may provide us some hints on the mechanisms of wave packet formation.
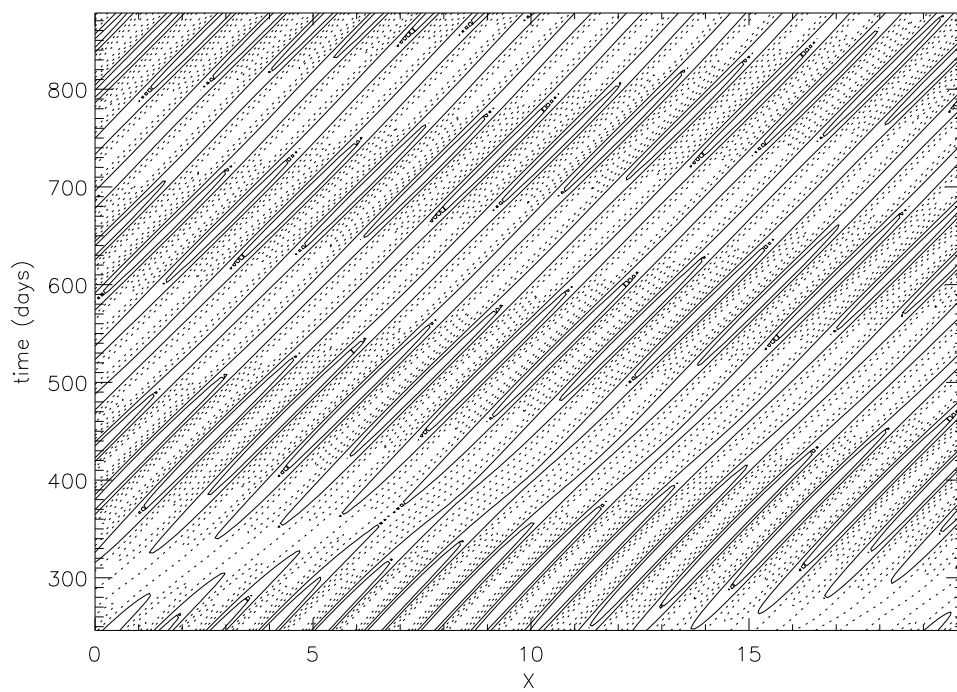
Figure 5: The longitude-time contour plot for the $\sin \frac{y}{N}$ mode of the upper layer stream-function with base functions specified in (13). The unit of x is again $2\pi\lambda$.

6 Concluding Remarks

This work attempts to construct truncated 2-layer QG models for the study of finite amplitude baroclinic waves. I find that models severely truncated in the meridional direction are capable of capturing essential features of the fully resolved model. This is an indication of small degrees of freedom in the y direction. Truncation (I) is capable of simulating the asymmetric life cycle of the eddies, although only to a small extent due to the inefficiency of the truncated model in simulating fine scalewave breaking events. Coherent wave packets are found for truncated models that are quasi-linear, but not for models with wave-wave interactions in the eddy evolution equations. Coherent wave packets are also found for untruncated models with a wide channel and with a Gaussian zonal wind shear profile, but not for models with a narrow channel and with a uniform shear. Understanding these two differences may shed some lights on the mechanisms of wave packet formation. I also note that some important aspects of the problem have not been explored in this study, including, for instance, the effects of the channel width and the effects of different shapes of zonal wind profile.

7 Acknowledgement

Appendix

Suppose that we take two eddy base functions $()' \sin \frac{my}{N}, ()' \sin \frac{ly}{N}$ so that

$$\psi'_M = A'_M \sin \frac{my}{N} + B'_M \sin \frac{ly}{N}$$

$$q'_M = \left(\frac{\partial^2 A'_M}{\partial x^2} - \frac{m^2 A'_M}{N^2}\right) \sin \frac{my}{N} + \left(\frac{\partial^2 B'_M}{\partial x^2} - \frac{l^2 B'_M}{N^2}\right) \sin \frac{ly}{N}$$

Now we calculate $J(\psi'_M, q'_M)$. The Jacobian of the $\sin \frac{my}{N}$ and the $\sin \frac{my}{N}$ terms is

$$\left\{ \frac{\partial A'_M}{\partial x}\left(\frac{\partial^2 A'_M}{\partial x^2} - \frac{m^2 A'_M}{N^2}\right)\frac{m}{N} - A'_M\left(\frac{\partial^3 A'_M}{\partial x^3} - \frac{m^2}{N^2}\frac{\partial A'_M}{\partial x}\right)\frac{m}{N} \right\} \frac{1}{2} \sin \frac{2my}{N} \qquad (16)$$

The x average of Eq. 16 vanishes as

$$\frac{\partial A'_M}{\partial x}\frac{\partial^2 A'_M}{\partial x^2} = \frac{1}{2}\frac{\partial(\partial A'_M/\partial x)^2}{\partial x}$$

$$A'_M\frac{\partial A'_M}{\partial x} = \frac{1}{2}\frac{\partial(A'_M)^2}{\partial x}$$

$$A'_M\frac{\partial^3 A'_M}{\partial x^3} = \frac{\partial}{\partial x}\left(A'_M\frac{\partial^2 A'_M}{\partial x^2}\right) - \frac{\partial A'_M}{\partial x}\frac{\partial^2 A'_M}{\partial x^2}$$

and
$$\overline{\frac{\partial()}{\partial x}}^{x} = 0$$

The same is true for the Jacobian of the $\sin\frac{ly}{N}$ and the $\sin\frac{ly}{N}$ terms. On the other hand, the x averages of the Jacobians of the $\sin\frac{my}{N}$ and the $\sin\frac{ly}{N}$ terms generally do not vanish and produce nonzero terms of the form $\overline{()}\sin\frac{(l-m)y}{N}$ and $\overline{()}\sin\frac{(l+m)y}{N}$. When projected onto the zonal mean base functions of the form $\overline{()}\cos\frac{ky}{N}$, we note that

$$\int_0^{N\pi} \sin\frac{iy}{N}\cos\frac{jy}{N}dy = \begin{cases} 0 & i-j \ is \ even \\ \frac{2Ni}{i^2-j^2} & i-j \ is \ odd \end{cases}$$

We also note that only changes in zonal mean components with odd k's change the total momentum. Therefore, if l-m is odd, the Jacobian terms have zero projection onto those components, and the momentum is automatically conserved. If l-m is even, the Jacobian terms have non-zero projection onto zonal mean components with odd k's. Total momentum would not be conserved unless all zonal mean components have zero momentum when integrated over the whole channel.

References

[1] W. J. Randel and J. L. Stanford, "The observed life cycle of a baroclinic instability," J. Atmos. Sci. **42**, 1364 (1985).

[2] A. J. Simmons and B. J. Hoskins, "The life cycles of some non-linear baroclinic waves," J. Atmos. Sci. **35**, 414 (1978).

[3] S. B. Feldstein and I. M. Held, "Barotropic decay of baroclinic waves in a two-layer beta-plane model," J. Atmos. Sci. **46**, 3416 (1989).

[4] E. K. M. Chang, "Downstream development of baroclinic waves as inferred from regression analysis," J. Atmos. Sci. **50**, 2038 (1993).

[5] S. Lee and I. M. Held, "Baroclinic wave packets in models and observations," J. Atmos. Sci. **50**, 1413 (1993).

[6] J. Pedlosky, *Geophysicsl Fluid Dynamics, 2nd ed.* (Springer-Verlag, New York, 1987).

[7] J. G. Esler, "Wave packets in simple equilibrated baroclinic systems," J. Atmos. Sci. **54**, 2820 (1997).